Published in final edited form as:
Colloids Surf B Biointerfaces. 2012 December 1; 100: 215–221. doi:10.1016/j.colsurfb.2012.05.012.

Antimicrobial activity of CdS and Ag_2S quantum dots immobilized on poly(amidoamine) grafted carbon nanotubes

Gururaj M. Neelgund[a], **Aderemi Oki**[a,*], and **Zhiping Luo**[b]

[a]Department of Chemistry, Prairie View A&M University, Prairie View, TX 77446, USA

[b]Microscopy and Imaging Center and Materials Science and Engineering Program, Texas A&M University, College Station, TX 77843, USA

Abstract

Herein we report the design of antimicrobial nanohybrids, *f*-MWCNTs-CdS and *f*-MWCNTs-Ag_2S developed by covalent grafting of cationic hyperbranched dendritic polyamidoamine (PAMAM) onto multiwalled carbon nanotubes (MWCNTs) and successive deposition of CdS and Ag_2S quantum dots (QDs). The CdS and Ag_2S QDs were *in-situ* deposited on PAMAM grafted MWCNTs instead of anchoring the pre-synthesized QDs. The fourth generation, amine terminated hyperbranched PAMAM was grafted on MWCNTs, which was achieved through repetitive reactions of Michael addition of methylmethacrylate to the surface amino groups and amidation of terminal ester groups with ethylenediamine. The covalent grating of PAMAM onto MWCNTs and the consecutive conjugation of CdS and Ag_2S QDs was characterized using Fourier transform infrared spectroscopy, elemental analysis, powder X-ray diffraction, Raman spectroscopy, transmission electron microscopy and energy dispersive spectroscopy. The antibacterial activity of *f*-MWCNTs-CdS and *f*-MWCNTs-Ag_2S nanohybrids was evaluated against *Escherichia coli, Pseudomonas aeruginosa and Staphylococcus aureus* and the results were compared with the activity of carboxylated MWCNTs, PAMAM grafted MWCNTs, PAMAM dendrimer, and CdS and Ag_2S QDs. It was found that the germicidal action of MWCNTs was enhanced by grafting of PAMAM, which was further improved with immobilization of CdS and Ag_2S QDs.

Keywords

Carbon nanotubes; Polyamidoamine; Cadmium sulfide; Silver sulfide; Antibacterial activity

1. Introduction

Carbon nanotubes (CNTs) with various unique physical and chemical properties have shown interesting applications in many fields, especially in the areas of nanomedicine [1,2]. For biomedical applications, pristine hydrophobic CNTs must be functionalized to afford water solubility and biocompatibility. While applications of CNTs are highly dependent on their surface molecules, hence, development of proper functional groups over CNTs is the most critical step to produce biocompatible CNTs. There are two major types of protocols used for functionalization of CNTs, viz., covalent reactions and non-covalent coating by amphiphilic molecules on CNTs. Among them, covalent grafting produces functionalized

*Corresponding author: Fax: +1-936-261-3117, aroki@pvamu.edu (A. Oki).

CNTs with high stability owing to strong binding of molecules. Various covalent functionalization reactions, such as oxidation of CNTs [3,4] and 1,3-dipolar cycloaddition [5] on the CNTs sidewalls, have been developed to produce water dispersible CNTs useful in biomedical applications such as drug delivery [2], antimicrobial agents [6,7] etc. In particular the antimicrobial activity of CNTs requires direct contact between CNTs and target microorganisms [7]. While, suspending the non-functionalized CNTs in water is extremely difficult, which does not provide enough contact between CNT and microorganism for disinfection. Accordingly, the antibacterial activity of CNTs could be exploited by coating CNTs on a reactor surface in contact with the pathogen laden water. Recently, antimicrobial agents developed on dendrimer functionalized CNTs have received particular interest due to combined properties of CNTs and dendrimers [6,8]. Dendrimers are highly branched molecules that possess unique properties including relatively large molecular size, narrow size distribution, well-defined globular structure, and ease of derivatization through the peripheral functional groups. These properties have attracted great interest in exploring their potential biomedical applications such as drug delivery, gene transfection, and imaging [9,10]. Recent research activities in this area also include the study of antimicrobial activities of dendrimer derivatives [11]. In most cases, dendrimers serve as carriers for biologically active agents by encapsulating them in the interior or more often, tethering them on its periphery. The development of dendrimers on the surface of CNTs is an effective way to produce hybrid materials with unprecedented properties. Poly(amidoamine) (PAMAM) is a class of highly branched, biocompatible dendrimer, which possess number of interesting characteristics and potential for biomedical applications, such as drug delivery [12–14] gene therapy[15,16] and *in- vivo* imaging [17]. Moreover there is a considerable current interest to use PAMAM as an antibacterial material [6].

Quantum dots (QDs) have been widely studied due to their unique optical properties and have become a novel functional platform in bio-analytical science and molecular imaging [18,19]. However, some reports showed that QDs exhibit cellular toxicity [20]. Areas of current interest include finding the ways to reduce the toxicity of QDs and enhance their biocompatibility. Some recent reports showed that dendrimers are ideal candidates for reduction of toxicity and enhancement of their biocompatibility [21,22].

In this contribution, we report the functionalization of multiwalled carbon nanotubes (MWCNTs) with fourth generation (G4), amine terminated PAMAM dendrimer based on the Michael addition and amidation. The dendritic PAMAM macromolecule constructed on MWCNTs was used as a platform for deposition of CdS and Ag_2S QDs. The covalent grafting of PAMAM on MWCNTs and subsequent deposition of CdS and/or Ag_2S QDs was characterized using Fourier transform infrared spectroscopy (FTIR), elemental analysis, Raman spectroscopy, powder x-ray diffraction (XRD), transmission electron microscopy (TEM), and x-ray energy dispersive spectroscopy (EDS). In addition, antibacterial activity of *f*-MWCNTs-CdS and *f*-MWCNTs-Ag_2S nanohybrids was evaluated against *Staphylococcus aureus (S. aureus)*, *Escherichia coli (E. coli)* and *Pseudomonas aeruginosa (P. aeruginosa)* bacterial pathogens and the results are compared with carboxylated MWCNTs, PAMAM grafted MWCNTs, PAMAM dendrimer, and CdS and Ag_2S QDs.

2. Experimental details

2.1. Materials

All the reagents were received from Sigma-Aldrich and used without further purification unless otherwise noted. For control experiment, fourth generation PAMAM dendrimer with ethylenediamine core was purchased from Sigma-Aldrich. All aqueous solutions were prepared with ultrapure water obtained from Milli-Q Plus system (Millipore).

Tetrahydrofuran (THF) used in the synthesis was dried over sodium benzophenone under nitrogen and freshly distilled prior to use.

2.2. Preparation of f-MWCNTs-QDs nanohybrids

The *f*-MWCNTs-CdS and *f*-MWCNTs-Ag_2S nanohybrids were prepared according to procedure reported by our group [23]. To be mention briefly, the acylated MWCNTs (MWCNTs-COCl) (prepared according to Ref. [24]) were dispersed in THF by sonication for 25 min and allowed to react with excess of ethylenediamine at 60 °C for 12 h. Then the fourth generation (G4) PAMAM dendrimer was constructed on MWCNTs by repeating the Michael addition of methylmethacrylate to the surface amino groups and amidation of terminal ester groups with ethylenediamine. The resulting PAMAM grafted MWCNTs (*f*-MWCNTs) were washed with methanol followed by DI water and dried under vacuum at 40 °C for 12 h. Then *f*-MWCNTs (20 mg) were dispersed in 20 mL methanol by sonication for 10 min and a solution of metal salt ($Cd(CH_3COO)_2$ or $AgNO_3$) (0. 01 mol L^{-1}) in 20 mL methanol was added. The resulting mixture was sonicated for an additional 15 mins and a freshly prepared solution of Na_2S in methanol (20 mL, 001. mol L^{-1}) was slowly added, followed by a combination of vigorous stirring and sonication for 15 mins. The suspension thus formed was stirred under ambient condition for 6 h. Thus obtained *f*-MWCNTs-QDs nanohybrids were centrifuged, subsequently washed with methanol and DI water, and dried in vacuum at 40 °C for 12 h. The overall procedure for preparation of *f*-MWCNTs-QDs nanohybrids is schematically depicted in Scheme I.

2.4. Preparation of CdS and Ag_2S QDs

The CdS and Ag_2S QDs were prepared according to similar procedure mentioned for *f*-MWCNTs-QDs nanohybrids without *f*-MWCNTs.

2.3. Antimicrobial Activity

The antimicrobial activity of carboxylated MWCNTs (MWCNTs-COOH), *f*-MWCNTs, *f*-MWCNTs-QDs nanohybrids, PAMAM dendrimer, and CdS and Ag_2S QDs were examined against the Gram-positive bacterium, *S. aureus* and the Gram-negative bacteria, *E. coli* and *P. aeruginosa*. All the tests were performed at Hygeia Laboratories Inc. Houston according to procedure reported earlier with slight modifications [8]. A brief description of the procedure is as follows, initially all the microorganisms were subcultured on Trypticase Soy Agar for 24 h and washed with phosphate buffered saline (PBS). Then the samples were diluted in PBS to provide a concentration of 20 μg/mL for tests. Subsequently, an amount of 20 μL of bacterial suspension in USP phosphate buffer (pH 7.2) was transferred to 1 mL of the prepared sample (20 μg sample/mL) in a test tube. The inoculated samples were kept in an incubator at 37 °C for 1 h with vortexing at every 15 min. After incubation, 1 mL of the sample was transferred to 9 mL of neutralizing broth and the mixture was left to stand in room temperature for 15 min. Then the tube was vortexed, and a series of 10-fold dilutions in neutralizing broth were prepared and plated out in Trypticase Soy Agar. The plates were incubated at 37 °C for 24 h and recorded the colony forming units (CFU). All the tests were performed in triplicate to ensure the reproducibility. The percentage of reduction (%R) in micro-organisms was calculated as,

$$\%R=(C_C-C_S/C_C)\,X\,100$$

where C_C (CFU) is the number of microbial colonies recorded on control and C_S (CFU) is the number of microbial colonies recorded on sample.

2.6. Characterization

FTIR spectra were obtained by Thermo-Nicolet IR 2000 spectrometer (KBr pellet) and Raman spectra were recorded by a Renishaw R-3000QE system at room temperature in the backscattering configuration using Argon ion laser with wavelength 785 nm. Powder XRD patterns were recorded at the rate of 3°/min on a Scintag X-ray diffractometer, model PAD X, equipped with a Cu Kα photon source (45 kV, 40 mA) and the elemental analysis was carried out using Thermo Scientific FLASH 2000 CHNS/O analyzer. TEM images were obtained with a JEOL 2010 microscope and EDS measurements were performed with a FEI Tecani F 20 system equipped with TEM.

3. Results and discussion

The covalent grafting of PAMAM dendrimer on MWCNTs and the functional groups exists on the periphery of *f*-MWCNTs and *f*-MWCNTs-QDs nanohybrids was analyzed by IR spectroscopy. The bands appeared at 1649 and 1516 cm^{-1} in the spectrum of *f*-MWCNTs (Fig. 1a) are corresponds to amide (-CO-NH-) I and II [25] and the broad band displayed at 3440 cm^{-1} is due to N-H stretching vibrations. The high intensity of N-H stretching band indicates the abundance of terminal amine groups in *f*-MWCNTs. In addition, the characteristic bands of MWCNTs were observed at 1380 cm^{-1} (C=C), 1110 cm^{-1} (-CH) and 837 cm^{-1} (C-H para-aromatic out of plane vibration) [26]. The absence of stretching vibrations of C=O around 1700 cm^{-1} in Fig. 1a demonstrates that -COOH groups on MWCNTs-COOH are completely converted into amide groups, confirming the successful grafting of PAMAM dendrimer onto MWCNTs through covalent linkages. All the characteristic bands appeared in *f*-MWCNTs were observed in the spectra of both *f*-MWCNTs-CdS (Fig. 1b) and *f*-MWCNTs-Ag_2S (Fig. 1c) nanohybrids, while the most obvious changes observed were position of bands and their intensity. The shifting of bands in nanohybrids indicates the existence of strong interaction between CdS or Ag_2S QDs and *f*-MWCNTs, which results for higher stability of *f*-MWCNTs-QDs nanobhybrids. To further characterize the grafting of PAMAM onto MWCNTs, elemental analysis was employed. The content of N found in *f*-MWCNTs was 6.42 wt% and that of C and H was 76.05 and 2.51 wt%, respectively. Among these elements, the content of N is contributed by PAMAM dendrimer, while C and H are derived from PAMAM and MWCNTs.

Fig. 2 shows powder XRD patterns of pristine MWCNTs (*p*-MWCNTs), *f*-MWCNTs and *f*-MWCNTs-QDs nanohybrids. The pattern of *p*-MWCNTs (Fig. 2a) displayed a peak corresponding to (0 0 2) plane of MWCNTs at 26.3° [27], while this characteristic peak in *f*-MWCNTs (Fig. 2b) was appeared at 26.1°. No drastic shift in the characteristic peak of MWCNTs was observed after functionalization with PAMAM, which indicates that, general structure of MWCNTs is retained in *f*-MWCNTs after functionalization also. The pattern of *f*-MWCNTs-CdS nanohybrid, shown in Fig. 2(c), exhibits a strong peak at 26.4° and a broad one around 47°. The former peak at 26.4° was resulted by overlapping of diffraction peaks from (1 1 1) plane of cubic CdS and (0 0 2) plane of MWCNTs. The following peak at 47° was supposed to be two peaks around 43.8° and 51.7°due to (2 2 0) and (3 1 1) planes of CdS, respectively (JCPDS 75-0581), whereas these peaks are diffused and broadened as the result of nanometric CdS crystallites. The pattern of *f*-MWCNTs-Ag_2S nanohybrid (Fig. 2d) displayed well distinguishable peaks indexed to (−1 0 1), (−1 1 1), (1 1 1), (−1 1 2), (1 2 0), (−1 2 1), (1 2 1), (−1 0 3), (0 3 1), (2 0 0), (−1 2 3), (−2 1 2), (0 1 4), (−2 1 3) and (−1 3 4) planes of acanthite structure of Ag_2S at 22.4°, 26.0°, 29.0°, 31.5°, 33.6°, 34.4°, 36.8°, 37.8°, 40.7°, 43.5°, 46.2°, 47.7°, 48.8°, 53.3° and 63.8°, respectively (JCPDS 14-0072). The XRD results shows that CdS and Ag_2S QDs deposited on *f*-MWCNTs are well ordered and the structure of MWCNTs has not destroyed by grafting of PAMAM.

Raman spectra of *p*-MWCNTs (Fig 3a), *f*-MWCNTs (Fig 3b), *f*-MWCNTs-CdS nanohybrid (Fig 3c) and *f*-MWCNTs-Ag_2S (Fig 3d) nanohybrid were recorded to characterize the grafting of PAMAM onto MWCNTs and successive deposition of CdS and Ag_2S QDs. All the spectra displayed three characteristic bands except *p*-MWCNTs (Fig 3a), which displayed two bands. The D-band, caused by induction of significant defects or disorder in the CNTs was observed at 1306 cm^{-1} (*p*-MWCNTs), 1310 cm^{-1} (*f*-MWCNTs), 1305 cm^{-1} (*f*-MWCNTs-CdS nanohybrid) and 1311 cm^{-1} (*f*-MWCNTs-Ag_2S nanohybrid) [28]. The G-band corresponding to crystallite graphitic structure was displayed at 1587 cm^{-1} (*p*-MWCNTs), 1577 cm^{-1} (*f*-MWCNTs), 1572 cm^{-1} (*f*-MWCNTs-CdS nanohybrid) and 1579 cm^{-1} (*f*-MWCNTs-Ag_2S nanohybrid). Moreover, the D_2-band (shoulder of the G band), which is also associated with the disorder and defects of CNTs was observed for *f*-MWCNTs, *f*-MWCNTs-CdS nanohybrid and *f*-MWCNTs-Ag_2S nanohybrid at 1604, 1603 and 1608 $cm^{-}1$, respectively [29]. The relative intensity ratio of D- and G-bands (*ID/IG* ratio) is extensively used as a measure of sidewall covalent derivatization or defect introduction in CNTs [30]. The ratio of *ID/IG* for *f*-MWCNTs (1.54) was found to be higher than *p*-MWCNTs (0.28), which reflect the successful grafting of PAMAM dendrimer onto MWCNTs through covalent linkage [31]. Further, the ratio of *ID/IG* for *f*-MWCNTs-CdS and *f*-MWCNTs-Ag_2S nanohybrids was found to be 1.17 and 2.53, respectively, which is different from the ratio calculated for *f*-MWCNTs (1.54), it indicates intrinsic disorder in MWCNTs is affected by the deposition of CdS and Ag_2S QDs [6].

TEM image of *f*-MWCNTs, shown in Fig. 4a reveals effective debundling of MWCNTs through deletion of van der Waals forces exists between MWCNTs owing to grafting of PAMAM dendrimer. Moreover, the existence of PAMAM on MWCNT is clearly observable in Fig. 4b, which demonstrates the efficiency of functionalization technique we followed. The presence of high density of CdS QDs in *f*-MWCNTs-CdS nanohybrid is easily recognizable in Figs. 4c and d. The CdS QDs immobilized on *f*-MWCNTs are non-spherical in shape and formed some clusters due to aggregation. In addition some kind of wrinkle patterns is observable in Figs. 4c and d, those are originated from residue of solvent used in the preparation of TEM sample. The Ag_2S QDs exists in *f*-MWCNTs-Ag_2S nanohybrid (Figs. 4c and d) are nearly spherical and efficiently dispersed. The diameter of Ag_2S QDs exists in *f*-MWCNTs-Ag_2S nanohybrid was found to be in the range of 2–19 nm, while calculation of the diameter of CdS QDs was not possible due clusters formed by aggregation. In general, both CdS and Ag_2S QDs are well immobilized on *f*-MWCNTs. There is no loosely bonded or free standing QD present in the void space, which shows that CdS or Ag_2S QDs incorporated in *f*-MWCNTs-QDs nanohybrids are stronger and stable. After formation of *f*-MWCNTs-QDs nanohybrids, the extended washing did not remove CdS or Ag_2S QDs from samples, which demonstrates existence of strong interaction between QDs and *f*-MWCNTs in *f*-MWCNTs-QDs nanohybrids. Further, the presence of CdS or Ag_2S QDs in *f*-MWCNTs-QDs nanohybrids was confirmed by EDS. The spectrum of *f*-MWCNTs-CdS nanohybrid (Fig. 5a) displayed prominent signals corresponding to Cd, S and C elements. Among these, signals Cd and S are generated from CdS QDs, while C is originated by *f*-MWCNTs. The atomic ratio of Cd to S calculated for *f*-MWCNTs-CdS nanohybrid is close to 1. The spectrum of *f*-MWCNTs-Ag_2S nanohybrid (Fig. 5b) demonstrated the existence of Ag, S and C elements in the sample. The atomic ratio of Ag to S calculated from Fig 5b is close to 2. Hence the EDS analysis confirms successful formation of *f*-MWCNTs-CdS and *f*-MWCNTs-Ag_2S nanohybrids through deposition of CdS and Ag_2S QDs over *f*-MWCNTs.

The bacterial inactivation or germicidal action of MWCNTs-COOH, *f*-MWCNTs, *f*-MWCNTs-QDs nanohybrids, PAMAM dendrimer, and CdS and Ag_2S QDs was evaluated and the results are illustrated in Fig. 6. The antibacterial data obtained for all samples are summarized in Table 1. For comparison, three control experiments were performed using

PAMAM dendrimer, and CdS and Ag_2S QDs and those data also included in Table 1. The MWCNTs-COOH has demonstrated bactericidal aptitude of 20±0.8, 26.8±1.1 and 14.7±0.5% for *E. coli*, *P. aeruginosa* and *S. aureus*, respectively. Under similar conditions, the microbe destruction of *f*-MWCNTs was 34.1±1.2, 60±1.8 and 22.8±0.9% for *E. coli*, *P. aeruginosa* and *S. aureus*, respectively. Hence, the antibacterial activity of *f*-MWCNTs is higher than MWCNTs-COOH. Further, the bacteria killing ability of *f*-MWCNTs-CdS nanohybrid was 87.2±4.1, 68.9±2.5 and 46.7±1.4% for *E. coli*, *P. aeruginosa* and *S. aureus*, respectively. While the efficacy of *f*-MWCNTs-Ag_2S nanohybrid was 97.8±2.1, 78.5±2.9 and 55.7±1.5% for *E. coli*, *P. aeruginosa* and *S. aureus*, respectively. As anticipated, *f*-MWCNTs are more effective than MWCNTs-COOH due to presence of PAMAM dendrimer and debundling of MWCNTs. Moreover, it is also known that PAMAM dendrimer with amine functional groups on their periphery, especially the primary amine group could penetrate through the bacterial cell membrane owing to their strong hydrogen bond donor characteristic properties toward biomolecules [32,33]. In this respect the inhibition activity of *f*-MWCNTs has governed by the presence of PAMAM dendrimer. Further the antibacterial activity of *f*-MWCNTs is significantly improved by the deposition of CdS or Ag_2S QDs. The activity of *f*-MWCNTs-Ag_2S nanohybrid is higher than *f*-MWCNTs-CdS nanohybrid, which shows that the bacterial reduction ability of Ag_2S QDs is better than CdS QDs. Overall, both *f*-MWCNTs-CdS and *f*-MWCNTs-Ag_2S nanohybrids exhibited remarkable bactericidal effect against all the three tested bacterial strains. The penetration of PAMAM dendrimer through bacterial cell membrane may help for the penetration of QDs also, which results for rapid destruction of bacterial cells. Although, the exact mechanism behind the bactericidal effect of *f*-MWCNTs-QDs nanohybrids is not known, it is expected that, when DNA molecules are in a relaxed state, the replication of DNA can be effectively conducted. While the DNA is in condensed form it loses its replication ability [34]. In the present study Ag_2S or CdS QDs penetrate into bacterial cell membrane, as a result the DNA molecule turns into a condensed form and inhabit its replication ability, which leads to distraction of bacterial cells. Anyway, to find the exact reason for observed enhancement in the activity of *f*-MWCNTs-QDs nanohybrids needs further detailed study.

A variation in antibacterial activity of all tested samples with the kind of bacteria was observed. For gram-positive bacterium, *S. aureus*, all samples showed a lower growth-inhibitory effect compared to gram-negative bacteria, *E. coli* and *P. aeruginosa* under identical conditions. To rationalize lower antimicrobial activity against *S. aureus*, we note that the antibacterial action of the samples may involve with disruption of cytoplasmic membrane of bacteria. For Gram-negative bacteria, *E. coli* and *P. aeruginosa*, the membrane consists of a thin (about 7–8 nm) periplasmic layer covered by an outer membrane containing negatively charged lipopolysaccharides (LPS) that facilitates binding of the dendrimer leading to membrane disruption [35]. On the other hand, the membrane of Gram-positive bacterium, *S. aureus* consisting of cross-linked peptidoglycan is thick (about 20–80 nm) and rigid, thus more difficult to be disrupted by the dendrimer. The observed lower germicidal activity against Gram-positive bacterium is in agreement with our previous results [8] and also the results reported by Yuan et al. [6] and Murugan and Vimala [36].

4. Conclusions

In summary, the antibacterial agents, *f*-MWCNTs-Ag_2S and *f*-MWCNTs-CdS were developed by functionalization of MWCNTs with covalent conjugation of NH_2-terminated PAMAM dendrimer and successive deposition of CdS and Ag_2S QDs. The complete conversion of -COOH groups exists in MWCNTs-COOH and the formation amide linkage were successfully achieved. The general structure of MWCNTs was retained after functionalization also and the CdS and Ag_2S QDs immobilized on *f*-MWCNTs were exists

in high density. Both *f*-MWCNTs and *f*-MWCNTs-QDs nanohybrids are stable and water dispersible. A stepwise enhancement in the antibacterial activity of MWCNTs was achieved through initial grafting of PAMAM and further immobilization of CdS and Ag_2S QDs. The *f*-MWCNTs-QDs nanohybrids are strong antimicrobial agents against gram-negative bacteria compare to gram-positive bacteria. These antibacterial agents might hold great potential in medicine, public transportation, home appliances, and sporting goods.

Acknowledgments

The authors acknowledge the support from NIH-NIGMS grant #1SC3GM086245 and the Welch foundation.

References

1. Liu Z, Tabakman S, Welsher K, Dai H. Carbon nanotubes in biology and medicine: in vitro and in vivo detection, imaging and drug delivery. Nano Res. 2009; 2:85–120. [PubMed: 20174481]
2. Bianco A, Kostarelo K, Partidos CD, Prato M. Biomedical applications of functionalised carbon nanotubes. Chem Commun. 2005:571–577.
3. Carson L, Kelly-Brown C, Stewart M, Oki A, Regisford G, Luo Z, Bakhmutov VI. Synthesis and characterization of chitosan-carbon nanotube composites. Mater Lett. 2009; 63:617–620. [PubMed: 20200591]
4. Rosca ID, Watari F, Uo M, Akaska T. Oxidation of multiwalled carbon nanotubes by nitric acid. Carbon. 2005; 43:3124–3131.
5. Tagmatarchis N, Prato M. Functionalization of carbon nanotubes via 1,3-dipolar cycloadditions. J Mater Chem. 2004; 14:437–439.
6. Yuan W, Guohua J, Che J, Qi X, Xu R, Chang MW, Chen Y, Lim SY, Dai J, Chan-Park MB. Deposition of silver nanoparticles on multiwalled carbon nanotubes grafted with hyperbranched poly(amidoamine) and their antimicrobial effects. J Phys Chem C. 2008; 112:18754–18759.
7. Kang S, Pinault M, Pfefferle LD, Elimelech M. Singlewalled carbon nanotubes exhibit strong antimicrobial activity. Langmuir. 2007; 23:8670–8673. [PubMed: 17658863]
8. Neelgund GM, Oki A. Deposition of silver nanoparticles on dendrimer functionalized multiwalled carbon nanotubes: synthesis, characterization and antimicrobial activity. J Nanosci Nanotechnol. 2011; 11:3621–3629. [PubMed: 21776746]
9. Bielinska A, Kukowska-Latallo JF, Johnson J, Tomalia DA, Baker JR. Regulation of *in vitro* gene expression using antisense oligonucleotides or antisense expression plasmids transfected using starburst PAMAM dendrimers. Nucleic Acids Res. 1996; 24:2176–2182. [PubMed: 8668551]
10. Svenson S, Tomalia DA. Dendrimers in biomedical applications-reflections on the field. Adv Drug Delivery Rev. 2005; 57:2106–2129.
11. Chen CZS, Cooper SL. Recent advances in antimicrobial dendrimers. Adv Mater. 2000; 12:843–846.
12. Kolhe P, Khandare J, Pillai O, Kannan S, Lieh-Lai M, Kannan RM. Preparation, cellular transport, and activity of polyamidoamine-based dendritic nanodevices with a high drug payload. Biomaterials. 2006; 27:660–669. [PubMed: 16054211]
13. Kurtoglu YE, Navath RS, Wang B, Kannan S, Romero R, Kannan RM. Poly(amidoamine) dendrimer-drug conjugates with disulfide linkages for intracellular drug delivery. Biomaterials. 2009; 30:2112–2121. [PubMed: 19171376]
14. Zhu S, Hong M, Tang G, Qian L, Lin J, Jiang Y, Pei Y. Partly PEGylated polyamidoamine dendrimer for tumor-selective targeting of doxorubicin: the effects of PEGylation degree and drug conjugation style. Biomaterials. 2010; 31:1360–1371. [PubMed: 19883938]
15. Shieh MJ, Peng CL, Lou PJ, Chiu CH, Tsai TY, Hsu CY, Yeh CY, Lai PS. Non-toxic phototriggered gene transfection by PAMAM-porphyrin conjugates. J Control Release. 2008; 129:200–206. [PubMed: 18541326]
16. Yang W, Cheng Y, Xu T, Wang X, Wen L. Targeting cancer cells with biotin–dendrimer conjugates. Eur J Med Chem. 2009; 44:862–868. [PubMed: 18550227]

17. Boswell CA, Eck PK, Regino CAS, Bernardo M, Wong KJ, Milenic DE, Choyke PL, Brechbiel MW. Synthesis, characterization, and biological evaluation of integrin $\alpha_v \beta_\varepsilon$ -targeted PAMAM dendrimers. Mol Pharmacol. 2008; 5:527–539.
18. Chan W, Nie S. Quantum dot bioconjugates for ultrasensitive nonisotopic detection. Science. 1998; 281:2016–2018. [PubMed: 9748158]
19. Cui D, Han Y, Li Z, Song H, Wang K, He R, Liu B, Liu H, Bao C, Huang P, Ruan J, Gao F, Yang H, Cho HS, Ren Q, Shi D. Fluorescent magnetic nanoprobes for in vivo targeted imaging and hyperthermia therapy of prostate cancer. Nano Biomed Eng. 2009; 1:61–74.
20. Derfus A, Chan W, Bhatia S. Probing the cytotoxicity of semiconductor quantum dots. Nano Lett. 2004; 4:11–18.
21. Pan B, Cui D, Sheng Y, Ozkan C, Gao F, He R, Li Q, Xu P, Huang T. Dendrimer-modified magnetic nanoparticles enhance efficiency of gene delivery system. Cancer Res. 2007; 67:8156–8163. [PubMed: 17804728]
22. Li Z, Huang P, He R, Lin J, Yang S, Zhang X, Ren Q, Cui D. Aptamer-conjugated dendrimer-modified quantum dots for cancer cell targeting and imaging. Mater Lett. 2010; 64:375–378.
23. Neelgund GM, Oki A. Photocatalytic activity of CdS and Ag_2S quantum dots deposited on poly(amidoamine) functionalized carbon nanotubes. Appl Catal B: Environ. (In Press).
24. Neelgund GM, Olurode K, Luo Z, Oki A. A simple and rapid method to graft hydroxyapatite on carbon nanotubes. Mater Sci Eng C. 2011; 31:1477–1481.
25. Zhang B, Chen Q, Tang H, Xie Q, Ma M, Tan L, Zhang Y, Yao S. Characterization of and biomolecule immobilization on the biocompatible multi-walled carbon nanotubes generated by functionalization with polyamidoamine dendrimers. Colloids Surf, B: Biointerfaces. 2010; 80:18–25. [PubMed: 20542415]
26. Sun ZP, Zhang XG, Liang YY, Li HL. Highly dispersed Pd nanoparticles on covalent functional MWNT surfaces for methanol oxidation in alkaline solution. Electrochem Comm. 2009; 11:557–561.
27. Neelgund GM, Oki A. Pd nanoparticles deposited on poly(lactic acid) grafted carbon nanotubes: Synthesis, characterization and application in Heck C–C coupling reaction. Appl Catal A: Gen. 2011; 399:154–160. [PubMed: 21731192]
28. Eklund PC, Holden JM, Jishi RA. Vibrational modes of carbon nanotubes; spectroscopy and theory. Carbon. 1995; 33:959–972.
29. Datsyuk V, Kalyva M, Papagelis K, Parthenios J, Tasis D, Siokou A, Kallitsis I, Galiotis C. Chemical oxidation of multiwalled carbon nanotubes. Carbon. 2008; 46:833–840.
30. Jia N, Lian Q, Tian Z, Duan X, Yin M, Jing L, Chen S, Shen H, Gao M. Decorating multi-walled carbon nanotubes with quantum dots for construction of multi-color fluorescent nanoprobes. Nanotechnology. 2010; 21:45606–45613.
31. He N, Chen Y, Bai J, Wang J, Blau WJ, Zhu J. Preparation and optical limiting properties of multiwalled carbon nanotubes with π-conjugated metal-free phthalocyanine moieties. J Phys Chem C. 2009; 113:13029–13035.
32. Sayed ME, Ginski M, Rhodes H. Transepithelial transport of polyamidoamine dendrimers across Caco-2 cell monolayers. J Control Release. 2002; 81:355–365. [PubMed: 12044574]
33. Tulu M, Aghatabay NM, Senel M, Dizman C, Parali T, Dulger B. Synthesis, characterization and antimicrobial activity of water soluble dendritic macromolecules. Eur J Med Chem. 2009; 44:1093–1099. [PubMed: 18657884]
34. Rangari VK, Mohammad GM, Jeelani S, Hundley A, Vig K, Singh SR, Pillai S. Synthesis of Ag/CNT hybrid nanoparticles and fabrication of their Nylon-6 polymer nanocomposite fibers for antimicrobial applications. Nanotechnology. 2010; 21:095102–095112. [PubMed: 20139493]
35. Wang L, Erasquin UJ, Zhao M, Ren L, Zhang MY, Cheng GJ, Wang Y, Cai C. Stability, antimicrobial activity, and cytotoxicity of poly(amidoamine) dendrimers on titanium substrates. ACS Appl Mater Interfaces. 2011; 3:2885–2894. [PubMed: 21774463]
36. Murugan E, Vimala G. Effective functionalization of multiwalled carbon nanotube with amphiphilic poly(propyleneimine) dendrimer carrying silver nanoparticles for better dispersability and antimicrobial activity. J Colloid Interface Sci. 2011; 357:354–365. [PubMed: 21377164]

Research Highlights

- Both the nanohybrids are water dispersible and good antimicrobial agents.
- NH_2-terminated PAMAM dendrimer was successfully constructed on MWCNTs through covalent linkage.
- PAMAM dendrimer was successfully replaced the van der Waals force exists in pristine MWCNTs.
- This method affords preservation of basic structure of MWCNTs after functionalization also.
- Germicidal action of Ag_2S QDs was found to be higher than CdS QDs.

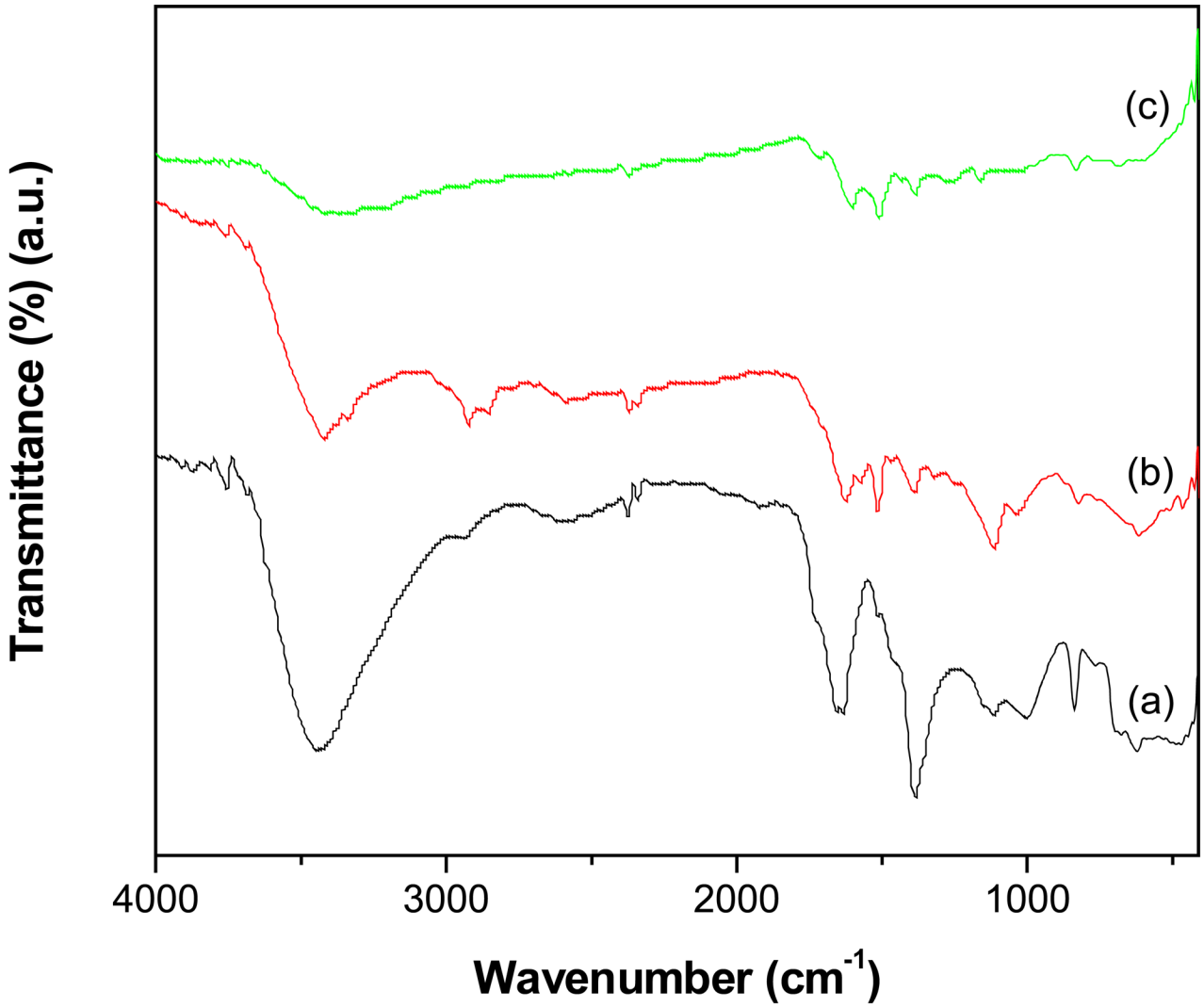

Fig. 1.
FTIR spectra of (a) *f*-MWCNTs (b) *f*-MWCNTs-CdS nanohybrid and (c) *f*-MWCNTs-Ag_2S nanohybrid.

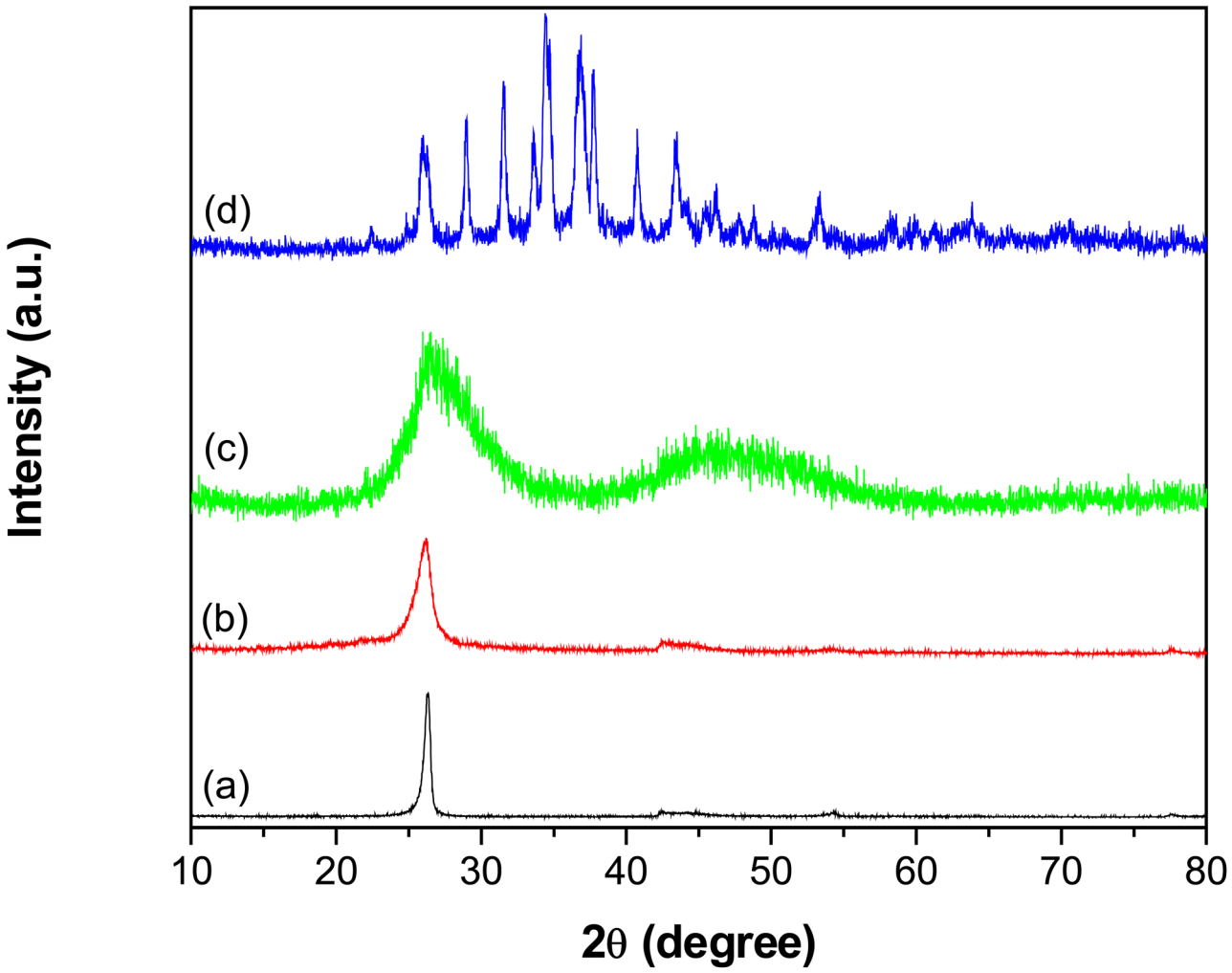

Fig. 2.
Powder XRD patterns of (a) *p*-MWCNTs (b) *f*-MWCNTs (c) *f*-MWCNTs-CdS nanohybrid and (d) *f*-MWCNTs-Ag_2S nanohybrid.

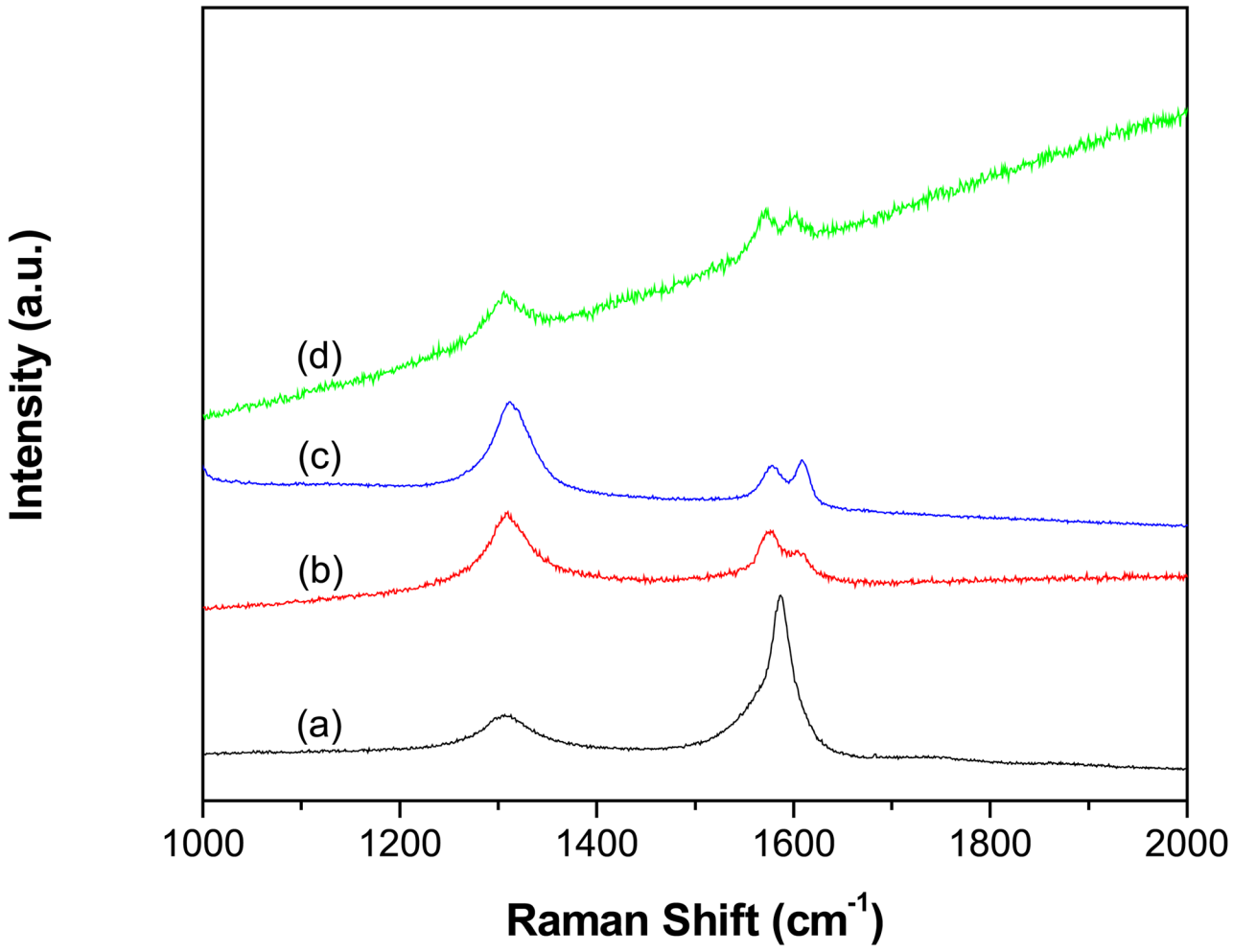

Fig. 3.
Raman spectra of (a) *p*-MWCNTs (b) *f*-MWCNTs (c) *f*-MWCNTs-CdS nanohybrid and (d) *f*-MWCNTs-Ag_2S nanohybrid.

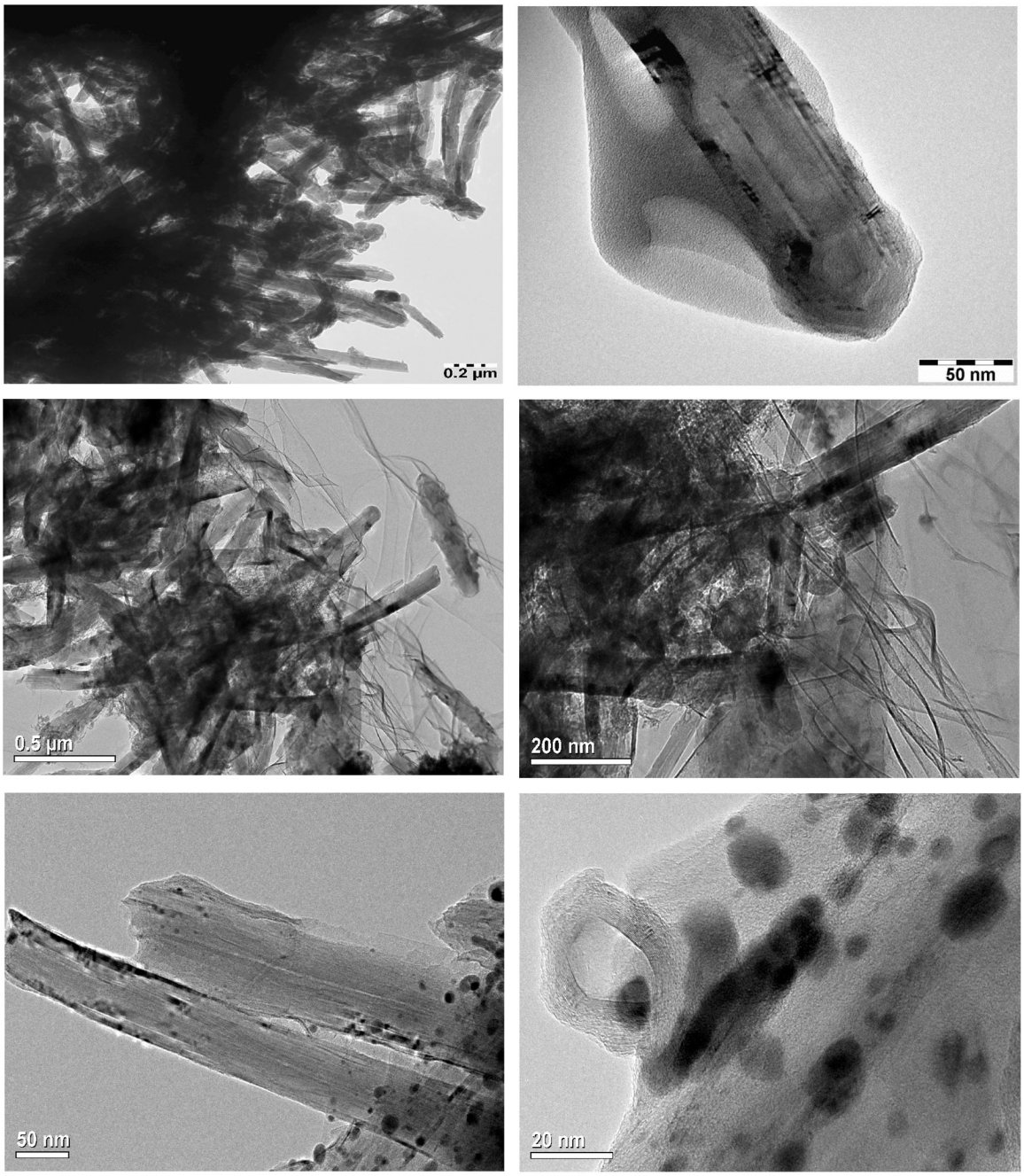

Fig. 4.
TEM images of (a,b) *f*-MWCNTs (c,d) *f*-MWCNTs-CdS nanohybrid and (e,f) *f*- MWCNTs-Ag_2S nanohybrid.

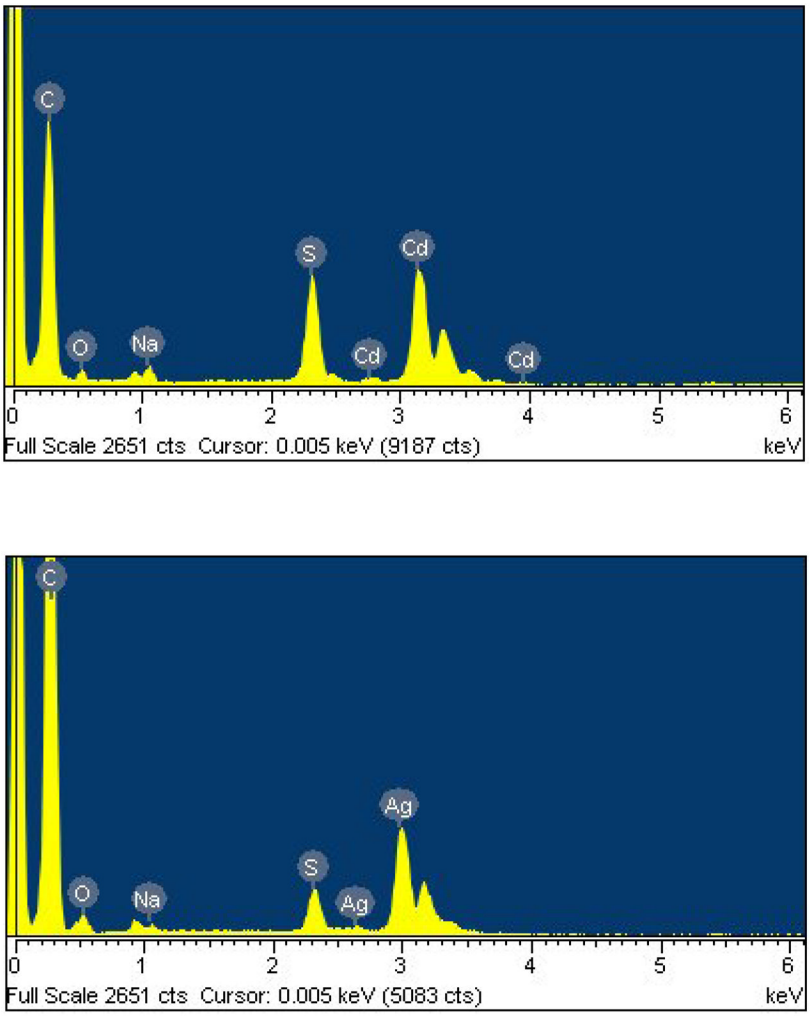

Fig. 5.
EDS of (a) *f*-MWCNTs-CdS nanohybrid and (b) *f*-MWCNTs-Ag_2S nanohybrid.

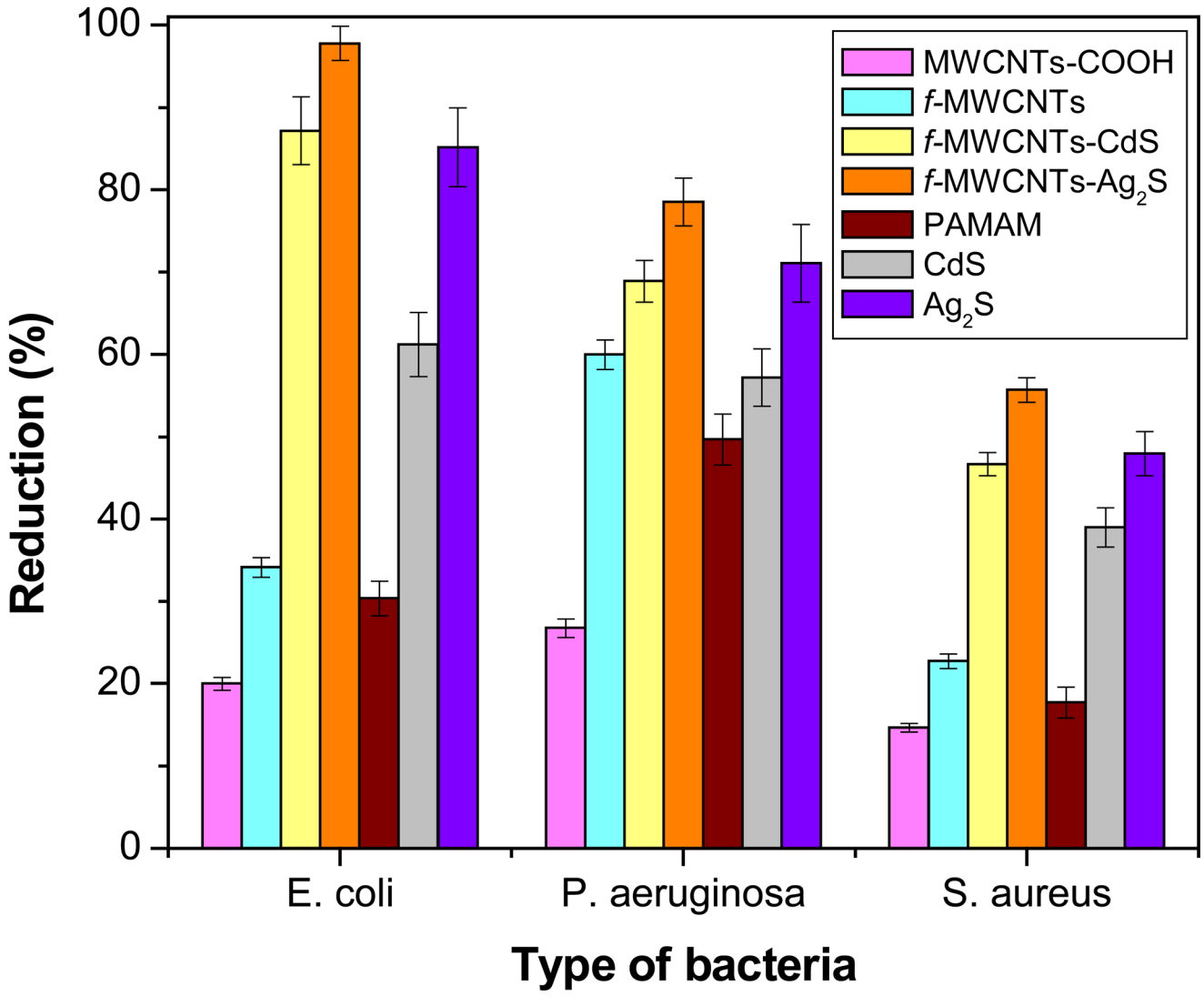

Fig. 6.
Antibacterial activity of MWCNTs-COOH, *f*-MWCNTs, *f*-MWCNTs-QDs nanohybrids, PAMAM dendrimer, and CdS and Ag_2S QDs (number of experimental repetitions, n =3).

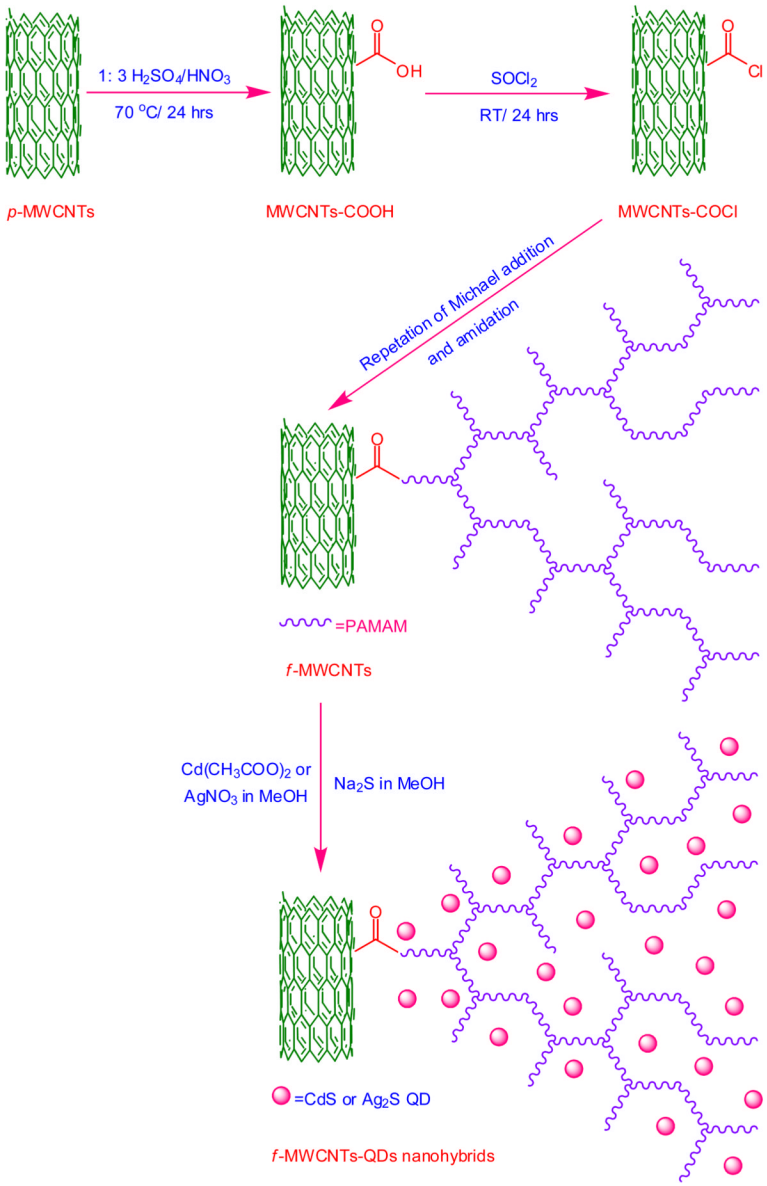

Scheme 1.
Preparation of *f*-MWCNTs-QDs nanohybrids.

Table 1

Antibacterial activity of MWCNTs-COOH, *f*-MWCNTs, *f*-MWCNTs-QDs nanohybrids, PAMAM dendrimer, and CdS and Ag_2S QDs.

	Reduction of bacteria (%)		
	E. coli	***P. aeruginosa***	***S. aureus***
MWCNTs-COOH	20±0.8	26.8±1.1	14.7±0.5
f-MWCNTs	34.1±1.2	60±1.8	22.8±0.9
f-MWCNTs-CdS	87.2±4.1	68.9±2.5	46.7±1.4
f-MWCNTs-Ag_2S	97.8±2.1	78.5±2.9	55.7±1.5
PAMAM dendrimer	30.4±2.1	49.7±3.1	17.7±1.9
CdS QDs	61.2±3.9	57.2±3.5	39±2.4
Ag_2S QDs	85.2±4.8	71.1±4.7	48±2.7